

Phase control of resonantly enhanced photoionization in an optically dense medium

David Petrosyan^{1,2,*} and P. Lambropoulos^{1,3,4}

¹*Institute of Electronic Structure & Laser, FORTH, P.O. Box 1527, Heraklion 71110, Crete, Greece*

²*Institute for Physical Research, ANAS, Ashtarak-2, 378410, Armenia*

³*Max-Planck-Institut für Quantenoptik, Hans-Kopfermann-Straße 1, D-85748 Garching, Germany*

⁴*Department of Physics, University of Crete, Crete, Greece*

(Received 7 August 2000; published 20 March 2001)

We present a self-consistent theory, as well as analytical and numerical results, for the three-photon–one-photon phase control of resonantly enhanced photoionization in an optically dense medium of xenon gas. We show that for an optically thick medium, the standard phase-control technique has a rather limited application since, independently of the initial relative phase between the two fields, over a very short scaled distance of propagation the medium tends to settle such a relative phase that exactly cancels the atomic excitation. Rather unusual results for an optically thin layer of atoms are also found.

DOI: 10.1103/PhysRevA.63.043417

PACS number(s): 32.80.Qk, 42.50.Gy, 32.80.Rm, 42.50.Hz

I. INTRODUCTION

The feasibility of the control of photoabsorption and its products through the external control of the relative phase of two electromagnetic fields of properly chosen frequencies has by now been demonstrated theoretically [1] as well as experimentally [2–4] in atoms and molecules. Typically, the system is exposed to the combination of a fundamental field and its third harmonic, so that control can be achieved via interference between the single- and three-photon absorption amplitudes, whose relative phase is employed as an external control mechanism to manipulate the interference. Many interesting issues [3–6] have been explored and clarified, establishing thus the idea as a useful tool, at least in the context of understanding intricate aspects of atomic and molecular photointeractions. In the vast majority of papers, however, theory and experiment have dealt only with single-atom situations. But, if the ideas are to be contemplated for applications, such as, e.g., separation of coherent and incoherent excitations of the species entering chemical reactions [7] or laser-induced catalyst [8], the issue of propagation of radiation through the medium is crucial. Depending on the density of the medium, propagation is known to affect the phase of the field, which in the present context is apt to have profound effects on the very process to be controlled.

To the best of our knowledge, this issue has been raised and investigated up to a point by Chen and Elliott [9] who have presented experimental data along such lines as well as an interpretation in terms of rate equations. Their study showed evidence of nonlinear coupling of the type discussed in the sections to follow and called for “more rigorous techniques” in the approach to this basic problem. We have in fact undertaken such an approach [10] and it is the purpose of this paper to present a complete account of the formal theory, as well as analytic (whenever possible) and numerical calculations, demonstrating that propagation does indeed have a profound influence on the whole process.

Before embarking on the technical aspects of this paper, it may be useful to remind the reader that the issue of coherent control through the relative phase of two fields is intimately related to previous work dating back 20 or more years ago that was stimulated by, unexpected at that time, cancellation effects in the process of third harmonic generation [11–13]. Specifically, it was noticed that in experiments involving third harmonic generation via three-photon resonance with a bound state, the inevitably present ionization from that state was practically canceled beyond a certain gas pressure, while the simultaneously generated third harmonic was not. The explanation turned out to be that the generated harmonic caused a single-photon transition to the resonant intermediate state, which interfered destructively with the three-photon transition due to the pump radiation [13–16]. The effect of the pressure was to produce the relative phase difference between the two fields that was necessary for destructive interference. The initial theoretical literature on what is now referred to as phase control does not reflect awareness of those earlier issues. But the papers reporting the initial experimental results by Elliott and collaborators definitely indicate detailed awareness of the prehistory of the underlying effects. It can be said that in a real sense, part of the process was turned around. Instead of relying on the internally generated third harmonic, Chen *et al.* [2] submitted the atom to a combination of pump radiation and its third harmonic generated prior to entering the cell with the system whose ionization was to be controlled by externally adjusting the relative phase of the two fields.

Propagation effects, essential in phase matching, were of relevance in the early experiments. They were also shown to be of relevance in later generalizations [17–19] of those cancellation effects. Related theoretical approaches had been developed, but had essentially stopped at the level of either weak-field treatment of the Maxwell-Bloch equations, or rate equations, as they had appeared to be sufficient at the time. Thus the chief motivation in the present work was to provide a more general approach, beyond rate equations; an approach which, as shown in Sec. III, recaptures the rate equations as a special case.

We have chosen to address here the basic system involv-

*Present address: Chemical Physics Department, Weizmann Institute of Science, Rehovot 76100, Israel.

ing a resonance with a bound state, which has served as an experimental and theoretical benchmark for the study of coherent control in the single-atom context. It is then natural to first examine the issue of propagation in the same context, which as we shall see involves a few surprises. Further issues involving continua and autoionizing states need to also be addressed from the perspective of propagation on which we expect to report in forthcoming papers.

We have structured the paper as follows: In Sec. II we formulate a self-consistent theory that governs the time and space evolution of the fields propagating in the atomic medium as well as the atomic response to those fields. The fields are described in the semiclassical formalism through the Maxwell equations and the medium in terms of the density matrix. On the basis of the developed mathematical formalism there, we present in Sec. III analytical results obtained in the rate approximation. The conditions of validity of this approximation are discussed emphasizing the experimental situations that can not be handled by this approach. Section IV is devoted to the exact numerical calculations performed for various initial conditions without making use of either the weak-field or rate approximations. Our conclusions are summarized in Sec. V.

II. FORMULATION

We examine the propagation of a bichromatic electromagnetic field E through an optically dense medium consisting of Xe gas. This electric field is a function of time t and space coordinate z and is composed of the fundamental and its third harmonic fields that have the same (linear) polarization and angular frequencies ω_f and $\omega_h = 3\omega_f$, respectively. It is expressed as

$$E(z,t) = \frac{1}{2} [E_f e^{i(k_f z - \omega_f t)} + E_h e^{i(k_h z - \omega_h t)} + \text{c.c.}], \quad (1)$$

where $E_j = \mathcal{E}_j e^{-i\phi_j}$, $j=f,h$, with \mathcal{E}_j and ϕ_j the slowly varying in time and space real amplitude and phase of the corresponding field, and $k_j = \omega_j n_j c^{-1}$ with $n_j \equiv n(\omega_j)$ the refractive index of the host medium at frequency ω_j . The electric field (1) induces the polarization

$$P(z,t) = \frac{1}{2} [P_f e^{i(k_f z - \omega_f t)} + P_h e^{i(k_h z - \omega_h t)} + \text{c.c.}], \quad (2)$$

where $P_j = \mathcal{P}_j e^{-i\phi_j}$ is the slowly varying in time and space field-induced medium polarization at frequency ω_j . Although in our present treatment, the host medium is the vacuum with a constant refractive index $n(\omega) = 1$, and thus $k_h = 3k_f$, for the sake of generality, e.g., presence of a buffer gas, we shall explicitly keep in the formalism the dependence on the refractive index. As shown in Fig. 1, the frequencies $\omega_{h,f}$ are chosen so that one harmonic and three fundamental photons are at near resonance with the transition from the ground state $|5p^6 \ ^1S_0\rangle \equiv |1\rangle$ to the $|6s[3/2]_1\rangle \equiv |2\rangle$ state of Xe. Further two-photon transition due to the strong fundamental field (with an intermediate near-resonant $|4f[3/2]_2\rangle$ state), or one-photon transition due to the har-

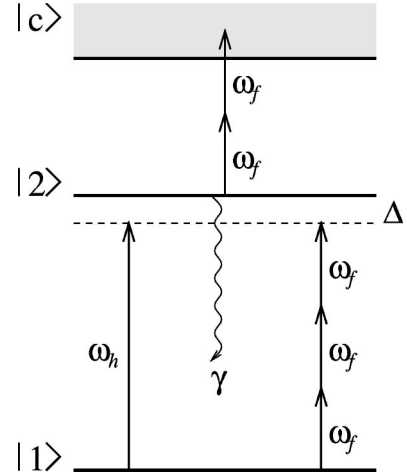


FIG. 1. Energy levels of Xe atom interacting with two electromagnetic fields. (Note that one fundamental photon cannot go into continuum.)

monic field lead to the ionization continuum (states $|c\rangle$) of the atom. As we intend to explore the intensities of the fields for which one- and three-photon transition amplitudes between the states $|1\rangle$ and $|2\rangle$ are of comparable magnitude (ideally equal) so as to maximize the modulation depth, the transition $|2\rangle \rightarrow |c\rangle$ would be dominated by the two-photon process and the one-photon ionization can be neglected. As for the polarization P_h at the frequency of the harmonic field, this simplification is further justified if one takes into account that the dipole matrix element between two bound states (i.e., $|1\rangle$ and $|2\rangle$) is, as a rule, much larger than that between a bound state and a smooth continuum ($|2\rangle$ and $|c\rangle$).

The situation we consider would correspond to an experimental setup where prior to entering the Xe-vapor cell, the strong pulsed fundamental field E_f from a laser is tripled in a nonlinear medium and then both the fundamental and its third harmonic pass through a dispersive medium through which the relative phase difference between the two fields can be controlled [2,3].

Beginning with the second-order wave equation for the field $E(z,t)$,

$$\frac{\partial^2 E}{\partial z^2} - \frac{n^2}{c^2} \frac{\partial^2 E}{\partial t^2} = \frac{1}{c^2 \epsilon_0} \frac{\partial^2 P}{\partial t^2}, \quad (3)$$

in the slowly varying during an optical cycle amplitude approximation, one neglects all second derivatives of E_j , $j=f,h$, and after projecting onto the corresponding mode function $\exp[i(\omega_j t - k_j z)]$, one arrives at

$$\frac{\partial E_j}{\partial z} + \frac{n_j}{c} \frac{\partial E_j}{\partial t} = \frac{1}{c \epsilon_0 n_j} \left[i \frac{\omega_j}{2} P_j - \frac{\partial P_j}{\partial t} \right]. \quad (4)$$

The most general approach to the calculation of the response of the medium is through the atomic-density matrix ρ , which obeys the master equation

$$\frac{\partial}{\partial t} \rho = -\frac{i}{\hbar} [H_{\text{atom}} + D, \rho], \quad (5)$$

where $H_{\text{atom}} = \sum_n \hbar \omega_n |n\rangle \langle n|$ is the free atomic Hamiltonian (the sum here and below is generalized to include summation over discrete and integration over continuum states: $\sum_n \rightarrow \sum_n + \int_c d\omega_c$) and $D = -\mu E$ is the atom-field interaction in the dipole approximation with μ being the electric-dipole operator. Introducing the rotating-wave approximation and adiabatically eliminating the continuum and all virtual (non-resonant) bound states connecting by the lowest-order paths, the states $|1\rangle$ and $|2\rangle$, the slowly varying density-matrix elements of these states $\sigma_{11} \approx \rho_{11}$, $\sigma_{22} \approx \rho_{22}$, and $\sigma_{21} \approx \rho_{21} \exp[i3(\omega_f t + \phi_f - k_f z)]$, are found to obey the following set of equations:

$$\frac{\partial}{\partial t} \sigma_{11} = \gamma \sigma_{22} - \text{Im} \left[\left(\frac{\mu_{12}^{(3)}}{\hbar} \mathcal{E}_f^3 + e^{i\theta} \frac{\mu_{12}}{\hbar} \mathcal{E}_h \right) \sigma_{21} \right], \quad (6a)$$

$$\frac{\partial}{\partial t} \sigma_{22} = -(\gamma + \gamma_{\text{ion}}) \sigma_{22} + \text{Im} \left[\left(\frac{\mu_{12}^{(3)}}{\hbar} \mathcal{E}_f^3 + e^{i\theta} \frac{\mu_{12}}{\hbar} \mathcal{E}_h \right) \sigma_{21} \right], \quad (6b)$$

$$\begin{aligned} \frac{\partial}{\partial t} \sigma_{21} = & - \left[\Gamma + i \left(\Delta - 3 \frac{\partial \phi_f}{\partial t} \right) + i \frac{s_1 - s_2}{2\hbar} \mathcal{E}_f^2 \right] \sigma_{21} \\ & + i \left(\frac{\mu_{21}^{(3)}}{2\hbar} \mathcal{E}_f^3 + e^{-i\theta} \frac{\mu_{21}}{2\hbar} \mathcal{E}_h \right) (\sigma_{11} - \sigma_{22}). \end{aligned} \quad (6c)$$

In these equations all the yet undefined symbols are γ the radiative decay rate of level $|2\rangle$,

$$\gamma_{\text{ion}} = \frac{1}{2\hbar^2} \mathcal{E}_f^4 \text{Im} \sum_c \frac{|\mu_{2c}^{(2)}|^2}{\omega_{c2} - 2\omega_f} = \frac{\pi |\mu_{2c}^{(2)}|^2}{2\hbar^2} \Big|_{\omega_c = \omega_2 + 2\omega_f} \mathcal{E}_f^4$$

the two-photon ionization rate from $|2\rangle$,

$$\Gamma = \frac{\gamma + \gamma_{\text{ion}}}{2} + \gamma_{\text{NR}}$$

the total relaxation rate of the atomic coherence, which contains also nonradiative dephasing γ_{NR} due to atomic collisions and laser-field fluctuations,

$$\begin{aligned} \mu_{2c}^{(2)} &= \frac{1}{2\hbar} \sum_m \frac{\mu_{2m} \mu_{mc}}{\omega_{m2} - \omega_f}, \\ \mu_{12}^{(3)} &= \frac{1}{(2\hbar)^2} \sum_{n,m} \frac{\mu_{1n} \mu_{nm} \mu_{m2}}{(\omega_{n1} - \omega_f)(\omega_f - \omega_{2m})} \end{aligned}$$

the effective two- and three-photon matrix elements for the fundamental field on the transitions $|2\rangle \rightarrow |c\rangle$ and $|1\rangle \rightarrow |2\rangle$, respectively,

$$s_1 = \frac{1}{\hbar} \sum_n \frac{\omega_{n1} |\mu_{1n}|^2}{\omega_{n1}^2 - \omega_f^2},$$

$$s_2 = \frac{1}{\hbar} \sum_m \frac{\omega_{2m} |\mu_{m2}|^2}{\omega_f^2 - \omega_{2m}^2}$$

the lowest-order ac Stark-shift coefficients (polarizabilities) of levels $|1\rangle$ and $|2\rangle$, $\mu_{nm} \equiv \langle n | \mu | m \rangle$ the (ordinary) matrix element of the electric-dipole operator μ , and $\omega_{nm} \equiv \omega_n - \omega_m$ is the energy difference between levels $|n\rangle$ and $|m\rangle$. Finally $\Delta = \omega_{21} - 3\omega_f = \omega_{21} - \omega_h$ is the detuning of both fields from the $|1\rangle \rightarrow |2\rangle$ transition resonance and $\theta = (\phi_h - 3\phi_f) - (k_h - 3k_f)z$ is their relative phase.

Consider now the polarization of the medium of atomic density N

$$P(z, t) = N \text{Tr}[\mu \rho] = N \sum_{n,m} \mu_{nm} \rho_{mn}. \quad (7)$$

In expanding the trace of this equation, we again follow the same procedure as in obtaining Eqs. (6), i.e., we use the adiabatic approximation to express all density-matrix elements that do not refer to the states $|1\rangle$ and $|2\rangle$ through the three main elements σ_{11} , σ_{22} , and σ_{21} . Equating the result with Eq. (2), after identifying and grouping together terms oscillating with the same frequencies, we obtain

$$\begin{aligned} \mathcal{P}_f &= 2N [\mathcal{E}_f (s_1 \sigma_{11} + s_2 \sigma_{22}) + 3\mu_{12}^{(3)} \mathcal{E}_f^2 \sigma_{21} \\ &+ i\pi \hbar^{-1} |\mu_{2c}^{(2)}|^2 \mathcal{E}_f^3 \sigma_{22}], \end{aligned} \quad (8a)$$

$$\mathcal{P}_h = 2N \mu_{12} \sigma_{21} e^{i\theta}. \quad (8b)$$

These equations, together with the Maxwell equation (4) and the atomic-density matrix equations (6), provide a complete self-consistent description of our system.

III. RATE APPROXIMATION

When dealing with pulse propagation problems, it is usually convenient to make the rate approximation that consists basically in setting the time derivative in the differential equation for σ_{21} equal to zero. This implies the assumption that the dephasing rate Γ of atomic coherence is greater than the rates of change of the (normalized) field amplitude and population difference $\sigma_{11} - \sigma_{22}$. Thus, for example, in an experiment with a relatively low power and large amplitude and/or phase fluctuations laser, when the total Γ dominates over the Rabi frequencies of the fields, the rate approximation is justified. As we show in the present section, this approximation allows for a simple analytical description of the system. If, however, a high-intensity narrow (Fourier limited) band laser output is required, the pulse duration is short so that in such experiments the conditions of validity of the rate approximation are typically not satisfied. Then the rigorous solution of the problem must be performed numerically which is the purpose of the next section.

For the analysis in this section, it is convenient to rewrite the density-matrix equations (6) transformed to the rotating frame of $(\omega_h t - k_h z)$, i.e., $\tilde{\sigma}_{11} \approx \rho_{11}$, $\tilde{\sigma}_{22} \approx \rho_{22}$, and $\tilde{\sigma}_{21} \approx \rho_{21} \exp[i(\omega_h t - k_h z)]$:

$$\frac{\partial}{\partial t} \tilde{\sigma}_{11} = \gamma \tilde{\sigma}_{22} - \text{Im} \left[\left(\frac{\mu_{12}}{\hbar} E_h^* + e^{i\delta k z} \frac{\mu_{12}^{(3)}}{\hbar} E_f^{*3} \right) \tilde{\sigma}_{21} \right], \quad (9a)$$

$$\frac{\partial}{\partial t} \tilde{\sigma}_{22} = -(\gamma + \gamma_{\text{ion}}) \tilde{\sigma}_{22} + \text{Im} \left[\left(\frac{\mu_{12}}{\hbar} E_h^* + e^{i\delta k z} \frac{\mu_{12}^{(3)}}{\hbar} E_f^{*3} \right) \tilde{\sigma}_{21} \right], \quad (9b)$$

$$\begin{aligned} \frac{\partial}{\partial t} \tilde{\sigma}_{21} = & -(\Gamma + i\tilde{\Delta}) \tilde{\sigma}_{21} + i \left(\frac{\mu_{21}}{2\hbar} E_h + e^{-i\delta k z} \frac{\mu_{21}^{(3)}}{2\hbar} E_f^3 \right) \\ & \times (\tilde{\sigma}_{11} - \tilde{\sigma}_{22}), \end{aligned} \quad (9c)$$

where $\delta k = k_h - 3k_f$ and $\tilde{\Delta} = \Delta + (s_1 - s_2)|E_f|^2/2\hbar$. Making the rate approximation, we obtain

$$\tilde{\sigma}_{21}(z) \approx \frac{d(z)}{\tilde{\Delta} - i\Gamma} \left(\frac{\mu_{21}}{2\hbar} E_h + e^{-i\delta k z} \frac{\mu_{21}^{(3)}}{2\hbar} E_f^3 \right), \quad (10)$$

with $d(z) = \tilde{\sigma}_{11} - \tilde{\sigma}_{22}$ the slowly varying population difference. Substitution of this equation into Eqs. (9a) and (9b) leads to the simple rate equations

$$\partial_t \tilde{\sigma}_{11} = \gamma \tilde{\sigma}_{22} - bd, \quad (11a)$$

$$\partial_t \tilde{\sigma}_{22} = -(\gamma + \gamma_{\text{ion}}) \tilde{\sigma}_{22} + bd, \quad (11b)$$

where

$$b = \frac{2\Gamma}{\tilde{\Delta}^2 + \Gamma^2} \left| \frac{\mu_{21}}{2\hbar} E_h + e^{-i\delta k z} \frac{\mu_{21}^{(3)}}{2\hbar} E_f^3 \right|^2$$

is the rate of stimulated transition from $|1\rangle$ to $|2\rangle$. Defining the real one- and three-photon Rabi frequencies $\Omega_{12} = \mu_{12} \mathcal{E}_h / 2\hbar$ and $\Omega_{12}^{(3)} = \mu_{12}^{(3)} \mathcal{E}_f^3 / 2\hbar$, respectively, it can be written in a form

$$b(\theta) = \frac{2\Gamma}{\tilde{\Delta}^2 + \Gamma^2} (\Omega_{12}^2 + \Omega_{12}^{(3)2} + 2\Omega_{12}\Omega_{12}^{(3)} \cos \theta) \quad (12)$$

that indicates most explicitly the interference arising from the variation of the relative phase θ [1,2]. Obviously, this effect is maximal if $\Omega_{12} \approx \Omega_{12}^{(3)} = \Omega$. Then Eq. (12) simplifies to

$$b(\theta) = \frac{4\Omega^2\Gamma}{\tilde{\Delta}^2 + \Gamma^2} (1 + \cos \theta), \quad (13)$$

which reveals that, with increasing relative phase θ from 0 to π , the stimulated transition rate decreases from its maximal value $b(0) = (8\Omega^2\Gamma)/(\tilde{\Delta}^2 + \Gamma^2)$, when the two Rabi frequencies interfere constructively, to $b(\pi) = 0$ when the interference is completely destructive.

Consider next the evolution of the field. To have comparable Rabi frequencies, the fundamental-field amplitude should be taken much larger than that of the harmonic field, since the three-photon transition-matrix element is much smaller than the single-photon one. Then, as the two fields

propagate, one can neglect the change of the amplitude and phase of the fundamental and concentrate only on the harmonic-field evolution. For the system we consider, this is indeed a very good approximation, as will be shown also quantitatively in Sec. IV. Consistently with the rate approximation, we assume further that the field varies significantly slowly for the time derivatives in Eq. (4) to be ignored. Thus, for the stationary propagation of the harmonic field, we have the equation

$$\frac{\partial E_j}{\partial z} = i \frac{\omega_h N \mu_{12} \tilde{\sigma}_{21}}{c \epsilon_0 n_h}. \quad (14)$$

Substituting here Eq. (10) and defining

$$a = \frac{N \omega_h \mu_{12} d(z)}{2\hbar c \epsilon_0 n_h} \frac{\tilde{\Delta} + i\Gamma}{\tilde{\Delta}^2 + \Gamma^2},$$

we obtain the differential equation for the harmonic field

$$\partial_z E_h = ia(\mu_{21} E_h + e^{-i\delta k z} \mu_{21}^{(3)} E_f^3). \quad (15)$$

Assuming $d(z)$ does not change significantly along z , which is quite reasonable in the weak-field limit when $\tilde{\sigma}_{22} \ll 1$ and $d(z) \approx \tilde{\sigma}_{11} \sim 1$, Eq. (15) can be solved analytically with the result

$$\begin{aligned} E_h(z) &= \frac{[(\delta k + a\mu_{21})E_h(0) + a\mu_{21}^{(3)}E_f^3]e^{ia\mu_{21}z} - a\mu_{21}^{(3)}E_f^3 e^{-i\delta k z}}{\delta k + a\mu_{21}}. \end{aligned} \quad (16)$$

For distances of propagation

$$z \gg \frac{1}{\text{Im}[a]\mu_{21}} = \frac{2\hbar c \epsilon_0 n_h (\tilde{\Delta}^2 + \Gamma^2)}{N \omega_h |\mu_{12}|^2 \Gamma d(z)} \equiv \zeta, \quad (17)$$

the term in front of the first exponent in the numerator of Eq. (16), which contains the initial field $E_h(0)$, is totally damped away and we are left with the simple expression

$$E_h(z) \approx -\frac{\mu_{21}^{(3)}}{\mu_{21}} E_f^3 e^{-i\delta k z}, \quad (18)$$

or, equivalently,

$$\mu_{21} \mathcal{E}_h(z) \approx \mu_{21}^{(3)} \mathcal{E}_f^3, \quad \theta \approx \pi. \quad (19)$$

This is a ‘‘z-steady’’ solution of Eq. (15) as one could have easily guessed even without solving it. Since $\text{Im}[a] > 0$, it is also a stable solution, i.e., small fluctuations of E_h decay away as z increases. The point for solving Eq. (15) is to establish condition (17), which tells us that, independently of the initial amplitude and phase, over a distance of several ζ , the harmonic field acquires such an amplitude and phase that its Rabi frequency equates with the Rabi frequency of the fundamental, the relative phase becomes π , and consequently, the stimulated transition rate b vanishes. With the

TABLE I. Atomic parameters used in the calculations.

Parameter	Value (in S.I. units)
γ	5.0×10^8
ω_{21}	1.2826×10^{16}
μ_{12}	4.324×10^{-30}
$\mu_{12}^{(3)}$	2.544×10^{-51}
$\mu_{2c}^{(2)}$	9.322×10^{-48}
s_1^a	1.40×10^{-40}

^a s_2 is set to zero since it is small by comparison and the continuum is smooth in the vicinity of $\omega_2 + 2\omega_f$.

parameters for Xe (see Table I) and in the weak (and monochromatic) field limit $\Gamma \sim \gamma \gg \Omega_{12}, \Omega_{12}^{(3)}, |\Delta|$, an estimate for ζ gives $\zeta \sim 6 \times 10^{10} N^{-1}$ cm, where N is measured in cm^{-3} . Increasing the detuning, intensity or bandwidth of the fields will result in larger values of ζ .

It is important to mention that the step leading from Eq. (16) to Eq. (18) assumes the condition $\delta k \ll \text{Re}[a]\mu_{21}$, i.e., the polarization for the harmonic field is conditioned by the resonant atomic response. Since in the present treatment, as well as in all works dealing with phase control, the two fields propagate collinearly, the buffer gas is absent and the three fundamental and one harmonic photons are near the atomic transition resonance, this condition is certainly satisfied. If there were an additional nonresonant contribution due to the presence of a buffer gas, or noncollinear propagation of the fundamental and harmonic fields, one should then look at the total phase mismatch $\delta k + a\mu_{21}$ in Eq. (16) that includes the resonant and nonresonant parts, and the ratio of these would determine the behavior of the system. This has been discussed in much detail in the paper by Elk *et al.* [19] where it was clearly established that only the resonant part results in cancellation that requires the smallness of δk [14].

We also stress that the analysis above corresponds to a plane wave rather than to a focused Gaussian beam geometry. However, since for not-extremely-low atomic densities ($N \geq 10^{12}$) the transient regime is very short ($\zeta \leq 0.06$ cm), the harmonic field settles to the steady-state value in a thin layer of interaction volume where the Gaussian beam can be well approximated by a plane wave and the result would be the same [19].

IV. NUMERICAL CALCULATIONS

Here we present and discuss the results of numerical solution of the equations derived in Sec. II. No rate approximation is made. This approach is fairly general and in the range of optical frequencies it is valid for pulse durations down to a fraction of a picosecond, i.e., as long as the pulse contains several tens of optical cycles. For the numerical simulations for Xe, we use the parameters calculated previously [5] via multichannel quantum defect theory. Those parameters, appropriately converted to conform to the present definitions, are collected in Table I.

For illustration purposes, it is desirable to have a maximally pronounced interference of the fundamental and harmonic fields. To obtain, for example complete cancellation at

$\theta = \pi$ when the Rabi frequencies of the two fields enter Eqs. (6) with opposite signs, it is obvious that Ω_{12} and $\Omega_{12}^{(3)}$ should overlap completely throughout the interaction time. Let the fundamental and harmonic fields have Gaussian temporal profiles

$$\mathcal{E}_j(t) = \mathcal{E}_j^{\max} \exp\left[-\frac{(t-t_{\max})^2}{\tau_j^2}\right], \quad j=f,h,$$

where $\mathcal{E}_j^{\max} \equiv \mathcal{E}_j(t=t_{\max})$ and τ_j are the peak amplitude and temporal width of the corresponding field. Then, for the complete overlapping of the Rabi frequencies throughout the interaction, these parameters should satisfy the relations

$$\mathcal{E}_h^{\max} = \frac{\mu_{12}^{(3)}}{\mu_{12}} (\mathcal{E}_f^{\max})^3, \quad \tau_h = \frac{\tau_f}{\sqrt{3}}. \quad (20)$$

The first of these conditions gives the equality of peak values of both Rabi frequencies, while the second one is responsible for the equality of their widths. The numerical factor $\sqrt{3}$ is due to the cubic dependence of the three-photon Rabi frequency on the field amplitude.

As a parameter corresponding to an observable in a real experiment, we define the ionization yield

$$Q(t) = [1 - \sigma_{11}(t) - \sigma_{22}(t)] = \int_0^t \gamma_{\text{ion}}(t') \sigma_{22}(t') dt', \quad (21)$$

where the last equality is obtained using Eqs. (6). If the ionization is measured at a long time after the two pulses are gone, which is what in reality happens, this equation simply reads as

$$Q \approx 1 - \sigma_{11}(t \rightarrow \infty), \quad (22)$$

which is the total probability of ionization produced by the fields.

A. Single-atom behavior

We consider first the behavior of a single atom interacting with the two fields without taking into account the influence of the atomic response on the phases and amplitudes of these fields. This situation corresponds to the interaction of the fields with an optically thin layer of medium at $z=0$.

In Fig. 2 we plot the ion yield Q , as a function of the relative phase θ for different intensities $I_f = c\epsilon_0 \mathcal{E}_f^2/2$ of the fundamental. In all cases, the harmonic-pulse duration $\tau_h = 1$ ns and the conditions (20) are satisfied. The detuning Δ is taken such that it compensates the relative Stark shift of levels $|1\rangle$ and $|2\rangle$ at the maximum t_{\max} of the pulse:

$$\Delta = -\frac{s_1 - s_2}{2\hbar} (\mathcal{E}_f^{\max})^2.$$

In this figure, for all intensities and the relative phase $\theta = \pi$, the ionization vanishes completely since the two Rabi frequencies interfere destructively and the second term in the

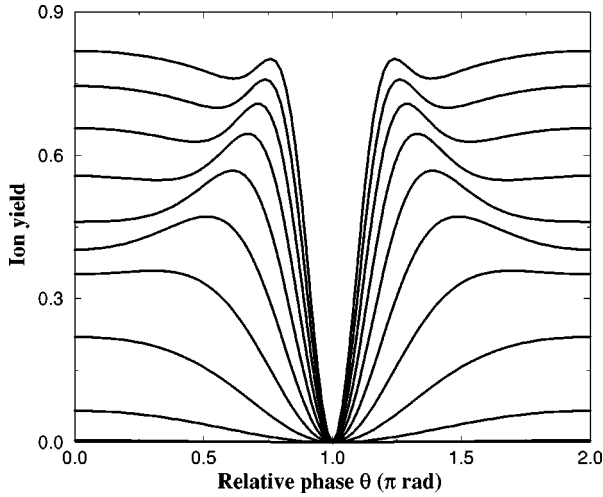


FIG. 2. Ion yield (22) vs relative phase θ for ten different peak intensities of the fundamental field: for the lowest curve $I_f^{\max} = 1 \times 10^{10}$ W/cm², then for every subsequent higher curve I_f is increased by 1×10^{10} W/cm².

right-hand side of Eq. (6a), responsible for the stimulated transition from $|1\rangle$ to $|2\rangle$ is equal to zero throughout the duration of the pulses. Consequently, the medium practically does not interact with the fields and the atoms are “trapped” in their ground state $|1\rangle$. For intensities $I_f \leq 3 \times 10^{10}$ W/cm², with increasing the relative phase θ from 0 to 2π the ionization profile follows approximately the $\cos \theta$ law, which is consistent with the results of Sec. III. For higher intensities of the fundamental, however, we obtain a surprising result; that is, the maximal ionization is observed at $\theta \neq 0, 2\pi$. This is because for intense and/or short pulses the pulsed nature of the fields begins to play an important role, and the rate approximation breaks down. Now the terms responsible for the stimulated transition in Eqs. (6), and consequently, the population σ_{22} of the upper atomic level reach maxima not at $\theta = 0, 2\pi, \dots$, as is illustrated in Fig. 3. It is also important that the ionization is caused by the same pulsed fundamental field that has the maximum at $t_{\max} = 2$ ns. Consequently, with variation of the relative phase, the shift of the moment of time at which σ_{22} reaches maximum with respect to t_{\max} is also essential for optimal ionization. Note that due to the increase of the ionization with increase of the intensity of the fundamental, the peak value of σ_{22} in Fig. 3, for the same θ 's, is higher in the case $I_f = 3 \times 10^{10}$ W/cm² than that for $I_f = 8 \times 10^{10}$ W/cm². One can see in Fig. 2, that increasing the intensity results in a narrower dip in the ionization profile and a shift of its peaks toward the values of θ that are closer to π . The numerical simulations also show that, while keeping the conditions (20) satisfied, with decreasing the pulse duration τ_f , the ion yield reduces and its peaks at $\theta \neq 0, 2\pi, \dots$ gradually disappear, which is equivalent to the decreasing of intensity since the total energy of the pulse lessens.

B. Pulse propagation

Let us turn now to the effects of propagation. The results presented below are obtained for a density of atoms N

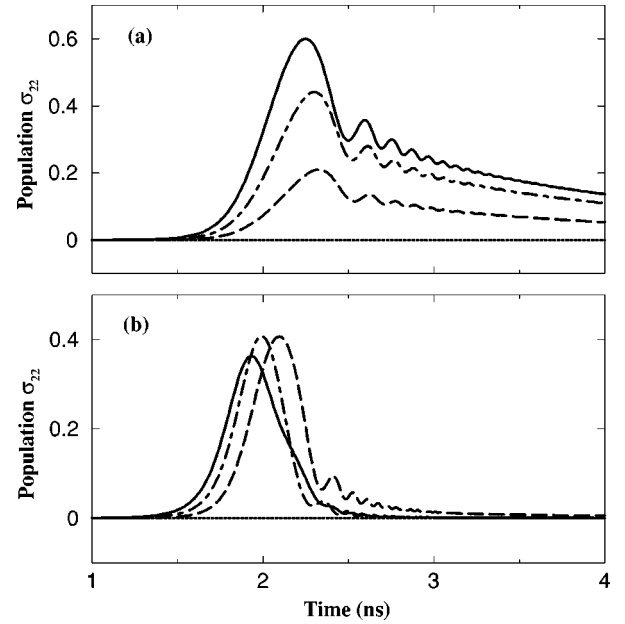


FIG. 3. Upper-level population σ_{22} as a function of time for (a) $I_f^{\max} = 3 \times 10^{10}$ W/cm², and (b) $I_f^{\max} = 8 \times 10^{10}$ W/cm². In both graphs, $\theta = 0$ (solid curve), $\theta = 0.5\pi$ (dot-dashed curve), $\theta = 0.72\pi$ (dashed curve), and $\theta = \pi$ (dotted curve).

$= 10^{13}$ cm⁻³. This, however, does not imply any limitation on the generality of the discussion since, as one can easily verify, the parameter $zN\Sigma$, where Σ is the beam cross section, is a propagation constant, and thus it is always possible to rescale the problem to any desired density and propagation length z . Meanwhile, for a density of atoms as low as the above, the nonradiative dephasings of the atomic coherence, i.e., the collisional relaxation, can safely be neglected. In all our simulations, conditions (20) are assumed at the entrance to the medium. As discussed above, in the case of initial phase difference $\theta(z=0, t) = \pi$, the atoms stay in the ground state and the medium appears to be “transparent” to both fields; neither the fundamental, nor the harmonic experience any remarkable distortion of their shapes or total energy $S_j(z) \propto \int dt |\mathcal{E}_j(z, t)|^2$, $j = f, h$, over distances of propagation z as large as ~ 50 cm. The change of the relative phase accumulated over this distance is only $\sim 10^{-3} \pi$ rad, which is due to the field-independent phase shift of the fundamental, given by the two terms (polarizabilities) in parentheses of Eq. (8a). Note, however, that since the excitation of the upper level $|2\rangle$ is canceled ($\sigma_{22} \sim 0$), only the term proportional to the polarizability s_1 of the ground state contributes.

Consider next the case $\theta(0, t) = 0$, i.e., at the entrance to the cell the two Rabi frequencies interfere constructively. The results corresponding to the parameters of Fig. 2 with $I_f^{\max} = 8 \times 10^{10}$ W/cm² are collected in Figs. 4 and 5. One can see in Fig. 4 that in the course of propagation, the relative phase θ (taken at the dynamic pulse maximum $t = t_{\max} + z/c$) grows rapidly and over a distance of the order of 1 cm reaches the value π at which the initial constructive interference turns to a destructive one. At the same time, the total energy of the harmonic pulse, after a small reduction over a short interval of z , begins to increase as a result of the

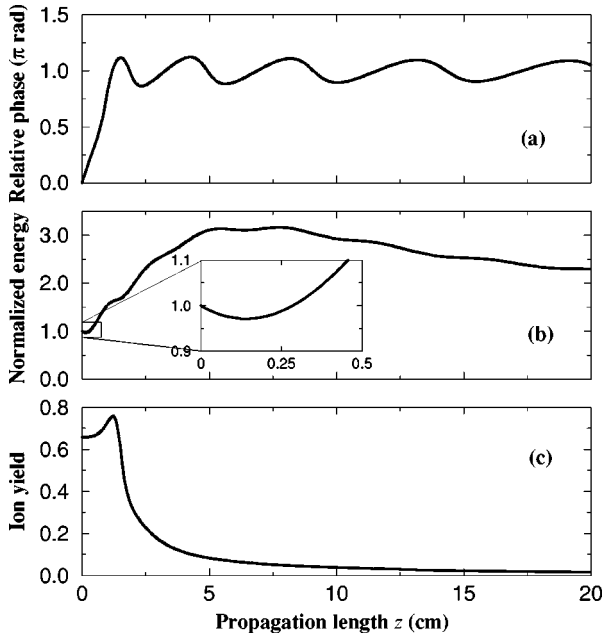


FIG. 4. Relative phase $\theta(z, t = t_{\max} + z/c)$ (a), normalized energy $S_h(z)/S_h(0)$ of the harmonic field (b), and ion yield $Q(z)$ (c) vs propagation length z for the case $I_f^{\max} = 8 \times 10^{10}$ W/cm 2 .

energy transfer from the strong fundamental field, in the parametric conversion process. This small reduction of the harmonic takes place only at the beginning of the propagation when the relative phase is still close to zero and the interference is constructive, in the process of excitation of atoms from the ground state $|1\rangle$ to the state $|2\rangle$, while the generated part of the harmonic field is out of phase with the fundamental approximately by π and continues to build up with slightly oscillating around the value π phase. It is important to mention that throughout the propagation, the am-

plitude and the phase of the fundamental field practically do not change. This is because the number of photons contained in that pulse exceeds by many (≥ 6) orders of magnitude the number of atoms the pulse interacts with over the distance of $z \leq 20$ cm. Comparing the three graphs of Fig. 4, one can see that with rising θ and S_h , the ionization probability first also grows, which is consistent with the previous discussion related to that intensity of the fundamental field. But as θ approaches π , the ion yield drops almost exponentially until $Q \approx 10\%$. This residual ionization that is present even at $\theta \approx \pi$ (and tends to 0 rather slowly) is caused by the fact that, because of the significant increase of the total energy of the harmonic field, the conditions (20) are not completely satisfied and the upper atomic level $|2\rangle$ acquires population due to that fraction of the generated field which exceeds the initial. Since the temporal widths of the pulses are less than the (radiative) relaxation time γ^{-1} of the polarization $\mathcal{P}_h \propto \sigma_{21}$, a significant fraction of the harmonic-pulse amplitude is generated behind the fundamental, as is seen in Fig. 5. In that figure, the frequency of rapid oscillations in the tail of the harmonic field corresponds to the (unperturbed) detuning Δ , since the fundamental pulse, that is responsible for the ac Stark shift of the atomic levels, is already gone. That part of the amplitude is then attenuated due to the atomic relaxation, therefore the total energy of the harmonic, after passing through a maximum at $z \sim 5-7$ cm, decays slowly back. Under these conditions, the leading part of the harmonic pulse that falls under the temporal shape of the fundamental is by $\theta \approx \pi$ out of phase with the latter and therefore the ionization vanishes, while the generated tail is continuously scattered by the atoms in the process of radiative decay. The oscillations of the relative phase around π are also slowly damped and the propagation reaches a ‘‘dynamic equilibrium.’’

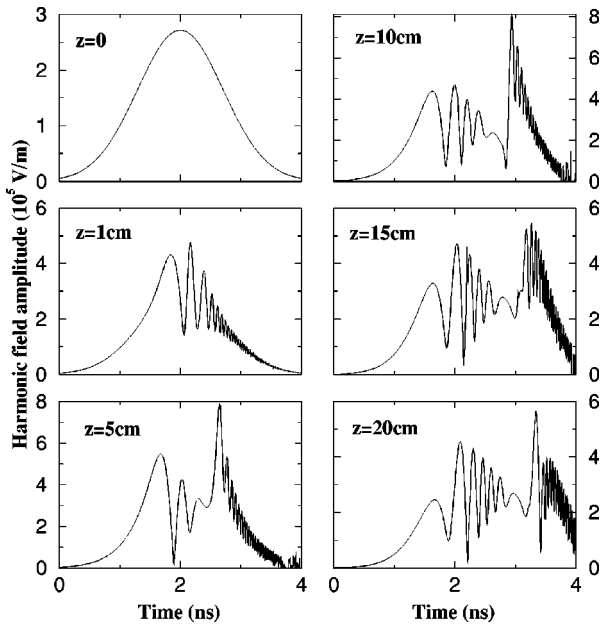


FIG. 5. Temporal profile of amplitude \mathcal{E}_h of the harmonic field at different z . All parameters are as in Fig. 4.

A similar behavior of the system is obtained for a range of intensities we have explored. As can be seen in Fig. 6, the main difference is that for weaker fields the ion yield drops to zero much faster as z increases and for $I_f^{\max} \leq 3 \times 10^{10}$ W/cm 2 it does not exhibit a maximum other than at $z=0$, which is consistent with the discussion in Sec. IV A.

We have also tested the case in which the harmonic field amplitude is zero at the entrance to the medium. As one can easily deduce from the results of this paper and has also been discussed in earlier work [19], the harmonic field is then generated in the medium in such a way as to cancel the excitation of level $|2\rangle$ and, consequently, the ionization that was due to the fundamental field alone at the beginning of propagation. We should note here that in [19] the analysis of the system was carried out only for the case in which the rate approximation is valid, and the question of what would happen to cancellation if rate approximation broke down was posed. Our present work establishes that the basic results of Ref. [19] remain valid under more general circumstances of short-pulse radiation, when the rate approximation is inadequate and one has to perform both time and space integration of the equations for the fields as well as for the atomic variables.

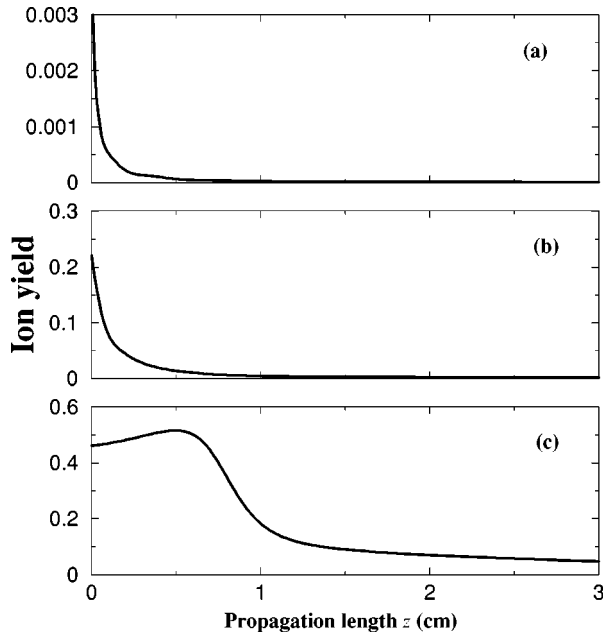


FIG. 6. Ion yield $Q(z)$ vs propagation length z for three different intensities of the fundamental: (a) $I_f^{\max} = 1 \times 10^{10}$ W/cm², (b) $I_f^{\max} = 3 \times 10^{10}$ W/cm², and (c) $I_f^{\max} = 6 \times 10^{10}$ W/cm².

V. CONCLUSIONS

We have shown theoretically that in an optically dense medium the propagation of a bichromatic electromagnetic field consisting of a fundamental and its third harmonic, with a preselected initial relative phase, has a profound effect.

Over a rather short scaled propagation distance, and independently of its initial value, the relative phase between the two components of the field settles to a value that makes the medium transparent to the radiation, thus precluding further excitation and consequently control. The scaled distance $zN\Sigma$ does of course involve the density of the species and the cross-section of the laser beam, which suggests some flexibility on the choice of these parameters. In any case, however, the actual length of the interaction region over which control can be active will be defined and limited by the combination of the above parameters, as well as by the geometry of the focused or unfocused laser beam.

The reader familiar with the effect of electromagnetically induced transparency (EIT) [20] might notice some similarities between the effects of propagation discussed in the present paper and those in the case of EIT. Although both effects are established in a coherent way and result in the transparency of the medium to two electromagnetic fields, the underlying physics is fundamentally different. The essence of EIT is a phenomenon of coherent population trapping resulting from the application of two laser fields to a three-level atomic system that creates a specific coherent superposition of the atomic states—the so-called “dark state”—that is stable against absorption of both fields. In that case, the two fields are not significantly altered by the medium and their relative phase is not important, while in the present work there is no specific stable superposition of the states since only two atomic levels are involved and it is the atomic response that modifies the relative phase of the fields in a way that the excitations from the ground level due to each field separately exactly cancel each other.

-
- [1] M. Shapiro, J. W. Hepburn, and P. Brumer, *Chem. Phys. Lett.* **149**, 451 (1988); C. K. Chan, P. Brumer, and M. Shapiro, *J. Chem. Phys.* **94**, 2688 (1991).
- [2] C. Chen, Y. Yin, and D. S. Elliott, *Phys. Rev. Lett.* **64**, 507 (1990); C. Chen and D. S. Elliott, *ibid.* **65**, 1737 (1990).
- [3] N. E. Karapanagioti, D. Xenakis, D. Charalambidis, and C. Fotakis, *J. Phys. B* **29**, 3599 (1996).
- [4] L. Zhu, K. Suto, J. A. Fiss, R. Wada, T. Seideman, and R. J. Gordon, *Phys. Rev. Lett.* **79**, 4108 (1997); L. Zhu, V. Kleiman, X. Li, S. Lu, K. Trentelman, and R. J. Gordon, *Science* **270**, 77 (1995), and references therein.
- [5] J. C. Camparo and P. Lambropoulos, *Phys. Rev. A* **55**, 552 (1997); **59**, 2515 (1999).
- [6] T. Nakajima and P. Lambropoulos, *Phys. Rev. Lett.* **70**, 1081 (1993); *Phys. Rev. A* **50**, 595 (1994); P. Lambropoulos and T. Nakajima, *Phys. Rev. Lett.* **82**, 2266 (1999); T. Nakajima, J. Zhang, and P. Lambropoulos, *J. Phys. B* **30**, 1077 (1997).
- [7] W. R. Garrett, Y. Zhu, L. Deng, and M. G. Payne, *Opt. Commun.* **128**, 66 (1996).
- [8] W. R. Garrett and Y. Zhu, *J. Chem. Phys.* **106**, L2045 (1997).
- [9] Ce Chen and D. S. Elliott, *Phys. Rev. A* **53**, 272 (1996).
- [10] D. Petrosyan and P. Lambropoulos, *Phys. Rev. Lett.* **85**, 1843 (2000).
- [11] R. N. Compton, J. C. Miller, A. E. Carter, and P. Kruit, *Chem. Phys. Lett.* **71**, 87 (1980); J. C. Miller, R. N. Compton, M. G. Payne, and W. W. Garrett, *Phys. Rev. Lett.* **45**, 114 (1980).
- [12] J. H. Glowia and R. K. Sander, *Phys. Rev. Lett.* **49**, 21 (1982).
- [13] D. J. Jackson and J. J. Wynne, *Phys. Rev. Lett.* **49**, 543 (1982); J. J. Wynne, *ibid.* **52**, 751 (1984); D. J. Jackson, J. J. Wynne, and P. H. Kes, *Phys. Rev. A* **28**, 781 (1983).
- [14] J. J. Wynne, in *Multiphoton Processes, Proceedings of 4th International Conference on Multiphoton Processes*, edited by S. J. Smith and P. L. Knight (Cambridge University Press, Cambridge, England, 1988), p. 318.
- [15] E. A. Manykin and A. M. Afanas'ev, *Zh. Éksp. Teor. Fiz.* **52**, 1246 (1967) [*Sov. Phys. JETP* **25**, 828 (1967)].
- [16] M. G. Payne and W. R. Garrett, *Phys. Rev. A* **26**, 356 (1982); **28**, 3409 (1983).
- [17] G. S. Agarwal and S. P. Tewari, *Phys. Rev. A* **29**, 1922 (1984).
- [18] M. G. Payne, W. R. Garrett, and W. R. Ferrell, *Phys. Rev. A* **34**, 1143 (1986); W. R. Garrett, W. R. Ferrell, M. G. Payne, and J. C. Miller, *ibid.* **34**, 1165 (1986).
- [19] M. Elk, P. Lambropoulos, and X. Tang, *Phys. Rev. A* **44**, R31 (1991); **46**, 465 (1992).
- [20] For a recent review, see S. E. Harris, *Phys. Today* **50** (7), 36 (1997).